Millimeter-wave two-dimensional imaging optical system for interferometer of the GAMMA 10 tandem mirror

doi: 10.1063/1.1473224

Millimeter-wave two-dimensional imaging optical system for interferometer of the GAMMA 10 tandem mirror

K. Watabe[a)]
National Metrology Institute of Japan, AIST, Tsukuba 305-8563, Japan

N. Oyama[b)] and A. Mase[c)]
Plasma Research Center, University of Tsukuba, Tsukuba 305-8577, Japan

K. Mizuno
Research Institute of Electrical Communication, Tohoku University, Sendai 980-8577, Japan

(Received 12 December 2001; accepted for publication 26 February 2002)

A millimeter-wave optical system for plasma diagnostics for measuring the two-dimensional distribution of electron density in the Tsukuba GAMMA 10 tandem mirror has been developed. Two-dimensional images of plasma density of a cross-sectional area of 83 mm×67 mm in the machine axis direction were successfully measured with the optical system. The position at which the present imaging system is installed corresponds to the plug region, and the plasma radius is relatively narrow (less than 100 mm). Information about the density in the area is valuable in the study of confining-potential formation. This optical system was developed for a millimeter-wave phase-imaging interferometer and was designed with the ray tracing method to reduce aberration. It was evaluated experimentally by measuring images of point sources and phase images of dielectric targets. The receiving optical system from the plasma to detector array was designed with a spatial resolution of 28.7 mm and a magnification of 0.30. Ray tracing indicated that the transverse spherical aberration was 78% of the sampling interval of 5.0 mm on an image plane and that even for the worst image point the distortion was 10% of the sampling interval. In the design of the optical system for plasma diagnostics, the off-focus effect due to plasma size (plasma diameter: 200 mm) with electron density profile is proposed and considered. © *2002 American Institute of Physics.* [DOI: 10.1063/1.1473224]

I. INTRODUCTION

Nuclear fusion occurring at high temperatures and high plasma densities has been extensively studied for use in power reactors. There is currently a considerable need for accurate measurements of electron density profiles in magnetically confined plasma with both high spatial and high temporal resolutions, as the profile is directly related to both the equilibrium and stability of the plasma. Millimeter-wave measurements are useful for plasma density diagnostics. Conventional interferometers rely on the use of a single detector with mechanical scanning or many detectors with multichannel optical chords to obtain density profiles. The use of multiple detectors in an imaging array,[1] however, does not require mechanical scanning or many optical components and makes real-time imaging possible in one plasma shot.[2,3]

Two-dimensional density distributions of plasma cross sections have been examined using a tomographic reconstruction on the TEXTOR tokamak,[4] the UCLA Microtor tokamak,[5,6] the H-1 helical,[7] the Microwave Tokamak Experiment,[8] and the TEXT-Upgrade,[9,10] but these results are the two-dimensional profiles of only one cross-sectional area. Since the density of the plug-cell plasma[11] varies axially as well as radially during the formation of the confining potential, it is essential to measure the time evolution of two-dimensional profiles in the machine axis direction of the plasma, i.e., three-dimensional profiles. The previous optical system[2,3] in the Tsukuba GAMMA 10 tandem mirror[11,12] was limited to two-dimensional imaging in the machine axis direction of ≈30 mm, since the probe beam scattered by the plasma continued expanding inside the plasma vessel without converging at the vacuum window, and additionally, ten lenses were required to arrange the beam. To overcome this restriction, we have designed a new optical system for the GAMMA 10 device to measure two-dimensional distribution in the machine axis direction of ≈200 mm. It consists of six mirrors and lenses in all and converges the scattered beam to pass the vacuum window. Parabolic and ellipsoidal mirrors installed inside the vacuum vessel ease the restriction of the view by the vacuum windows. Moreover, we considered the off-focus effect in the case of imaging deep plasma with electron density in the design of the new optical system. This implies that it is necessary to consider the effect of the depth of focus to design an optical system for plasma diagnostics. In the plasma measurements we used a two-dimensional imaging array consisting of 4×4, horn antennas, each with waveguides and beam-lead Schottky diode detectors.[3,13]

[a)]Author to whom correspondence should be addressed; on leave from Research Institute of Electrical Communication, Tohoku University, Sendai 980-8577, Japan; electronic mail: k.watabe@aist.go.jp
[b)]Present address: Japan Atomic Energy Research Institute, Naka-machi, Ibaraki-ken 311-0193, Japan.
[c)]Present address: Advanced Science and Technology Center for Cooperative Research, Kyushu University, Kasuga 816-8580, Japan.

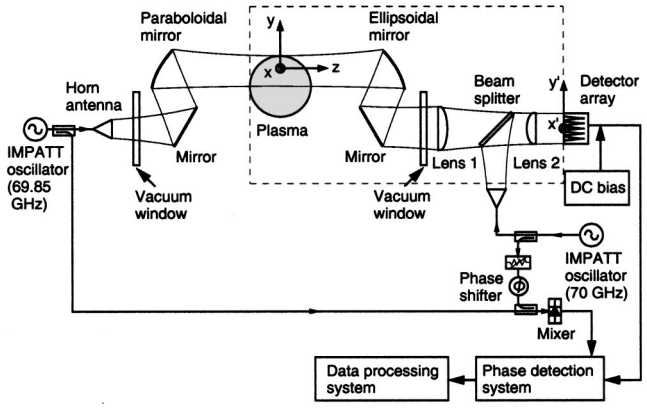

FIG. 1. Schematic of the millimeter-wave phase imaging system. The x axis coincides with the machine axis, where $x=0$ represents the midplane of the central cell. The y axis coincides with the radial direction of the plasma. The z axis coincides with the optical axis. x' and y' axes coincide on the image plane.

The design concept of this optical system will be applied to the large helical device in the National Institute for Fusion Science, Japan.[14] The imaging system still uses mechanical scanning of the imaging array but the number of scans necessary for taking a two-dimensional image is greatly reduced as a result of using the imaging array. Although most conventional millimeter-wave imaging has been one-dimensional imaging, two-dimensional imaging is the wave of the future. Millimeter-wave passive imaging has been attracting attention in recent years, and the design technique used to fabricate the optical system described here can be used for two-dimensional passive electron cyclotron emission imaging on plasmas[15] and millimeter-wave passive radiometric imaging for security measures such as contraband detection.[16]

In this article, the optical system for this measurement is discussed. Section II discusses the design of the receiving optical system, Sec. III discusses the experimental evaluation of the receiving optical system, and Sec. IV describes the use of the optical system to obtain two-dimensional line-density profiles.

II. DESIGN OF RECEIVING OPTICAL SYSTEM

Figure 1 shows the fundamental configuration of the optical system for a millimeter-wave two-dimensional phase-imaging interferometer. The object plasma for this interferometer is GAMMA 10 at the University of Tsukuba. The plasma diameter is 200 mm and its line density is expected to be on the order of 10^{12} cm^{-2} through which 70 GHz has been determined as the probe frequency. We assume that the density profile is axisymmetric. The probe beam is expanded in a parallel beam by a parabolic mirror resulting in efficient illumination of the upper half of the plasma. The two-dimensional area ($x-y$ plane) to be measured is 83 $\times 67$ mm. The receiving optical system has been designed to yield a specified spatial resolution and a magnification and to minimize the spherical aberration and the distortion. First the diameters of the optical system have been determined to obtain the desired resolution, which was calculated using Rayleigh's criterion for resolution[17]

$$\Delta x_R = 1.72 \frac{\lambda_0}{nD} z, \tag{1}$$

where Δx_R is the spatial resolution of an amplitude image in the case of coherent illumination, where it is assumed that two object points are illuminated by the same phase, n is the refractive index of the object (plasma), λ_0 is the vacuum wavelength, D is the aperture, and z is the distance between the object and the optical system. Then the distance between the optical system and the image plane, the effective F number, and the focal length needed to yield the desired magnification were calculated. Guidelines for the design of the optical system are to have low loss and to produce a spherical aberration smaller than the proper sampling interval for the 4×4 imaging array that allows exact reconstruction of a diffraction-limited image and the distortion less than 10% of the sampling interval. It was determined that an ellipsoidal mirror and two lenses would be necessary if these conditions were to be satisfied. The receiving optical system, shown inside the dashed lines in Fig. 1, from the plasma to the imaging array, has been designed with a spatial resolution of 28.7 mm, a magnification of 0.30, and an effective F number of 1.17 using the ray-tracing method to focus the plasma scattered beam on the array. The reason the effective F number is low is to obtain a high-resolution system by using a small diffraction-limited sampling interval. The ellipsoidal mirror and a plane mirror located inside the plasma vessel converge the scattered beam inside the vessel to pass the vacuum window of Teflon (21 cm long by 16 cm wide, with $n=1.46$), and the extended beam is focused through two low-density polyethylene ($n=1.51$) lenses to construct an image on the imaging array. In this receiving optical system an ellipsoidal mirror produces the magnification of 0.55 and the two lenses (diameters of 240 mm for No. 1 and 160 mm for No. 2, with focal lengths of 343 and 140 mm, respectively) yield a magnification of 0.55. An object plane located at the plasma center is 1.17 m away from the ellipsoidal mirror. The receiving optical system was designed to minimize the spherical aberration and the distortion on an image plane of 25×20 mm^2. The operation of the bending, which changes the shape of the lens on condition that the focal length is constant, has been carried out to minimize the spherical aberration. We used the shape factor as a parameter to represent the lens shape[17]

$$q = \frac{r_2 + r_1}{r_2 - r_1}, \tag{2}$$

where r_1 is the front-side radius of curvature, and r_2 is the back-side radius of curvature. The two aspheric lenses, whose curvatures were conic sections, were used to minimize the distortion. The curvatures of the two lenses were designed to obtain the optimum shape factor of -1.0 and 0.5 and the optimum conic constant of -0.9 and -1.5. The design of the optical system was checked by the three-dimensional ray tracing method. Figure 2 shows two-dimensional ray tracing of the receiving optical system. The refraction of the vacuum window of Teflon ($n=1.46$) and the beam splitter of low-density polyethylene ($n=1.51$) was also taken into account in the design. Ray tracing indicates

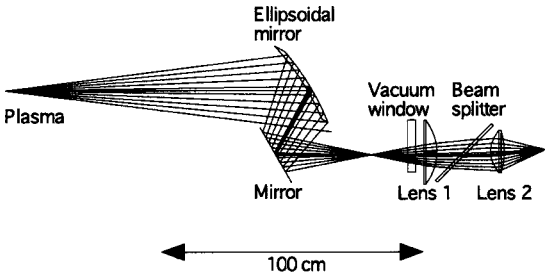

FIG. 2. Ray tracing of receiving optical system.

that transverse spherical aberration is 78% of the sampling interval and that even for the worst image point the distortion is 10% of the sampling interval. The effective F number of the whole system is 1.17, which determines the diffraction-limited sampling interval T_E of 5.0 mm on the imaging array. This was calculated by

$$f_0^E = \frac{n}{2\lambda_0 F_{\text{eff}}}, \tag{3}$$

$$T_E = \frac{1}{2 f_0^E}, \tag{4}$$

where n is the refractive index of the medium in which the image is formed.[18] The sampling interval corresponds to a plasma size of 16.7 mm. The image can be reconstructed by the Whittaker–Shannon sampling theorem.[19] Since the effective F number is small (1.17) and the diameter of lens No. 1 is large (240 mm), we must consider the effect of the depth of focus (off focus). Figure 3 shows the calculated diameter of the circle of confusion on the image plane as a function of off focus (the distance from the center of the plasma). Also shown is the electron density profile which is assumed to be parabolic. Using the data shown in this figure, the phase change of the integral of the electron density due to inferior resolution (increase of circle of confusion) has been calculated to be less than 10% of the ideal phase change. This

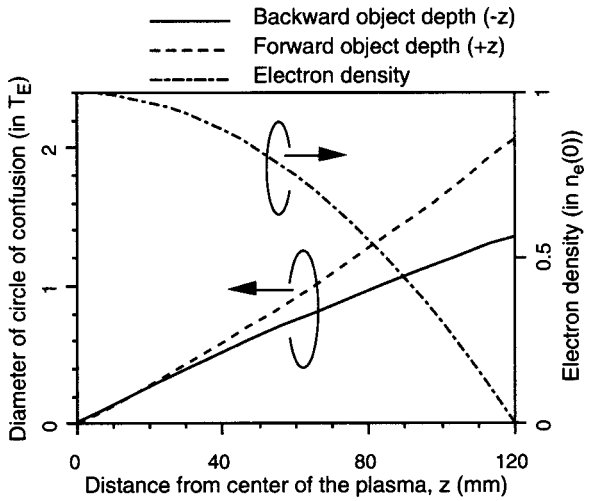

FIG. 3. Theoretical diameter of the circle of confusion as a function of the position of an object point in the plasma. The diameter is normalized by the detector interval. The electron density is also indicated. T_E is the sampling interval of 5.0 mm on the imaging array and $ne(0)$ is the electron density at the center of the plasma.

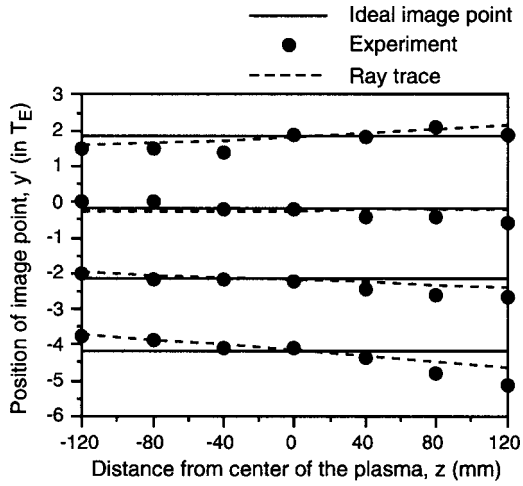

FIG. 4. Measured points of a point source as a function of the source position in a cross section of the plasma which corresponds to $x = 869$ cm. The solid lines are the position of the ideal image. The dashed lines are the position of the image obtained by the ray tracing method.

suggests that even if the image is off focus, it has little influence on the resultant phase image, since electron density at the edge of the plasma is low.

III. EXPERIMENTAL EVALUATION OF THE RECEIVING OPTICAL SYSTEM

The receiving optical system designed in Sec. III has been evaluated experimentally at 70 GHz. Figure 4 shows the measured points of a point source as a distance from the center of the plasma. The coordinates are shown in Fig. 1. The experimental results agree well with the results from the ray tracing method.

The system has been tested to provide diffraction-limited phase images using dielectric targets by the same method used by Young *et al.*[20] Figures 5(a) and 5(b) show the two-dimensional image of a Teflon plate 10.1 mm long, 10.1 mm wide, and 1.5 mm thick, with a refractive index of $n = 1.46$. The location of the Teflon plate corresponds to the west plug cell in the GAMMA 10 tandem mirror where the imaging system was installed. The solid curves in the figures show the theoretical phase shift as a continuous function of space, and the dashed curves were calculated (using the Whittaker–Shannon sampling theorem) from the data measured experimentally. The images have phases that drop below zero, because of the imaging of the targets with sharp edges over the resolution of the optical system. Although the measured data have errors of about $\pm 5°$ because of the readout error, the similarity of the experimental and calculated results for both phase shift and magnification verifies the validity of this two-dimensional imaging system.

IV. PLASMA MEASUREMENTS

The designed receiving optical system (Fig. 1) has been applied to measure the plasma line density profile in the GAMMA 10 at the University of Tsukuba. An IMPATT oscillator (Millitech, IDO-12-R27NBN) with a 500 mW output at 69.85 GHz was used as the probe beam. The probe beam was mixed with a longitudinal optical (LO) signal which was

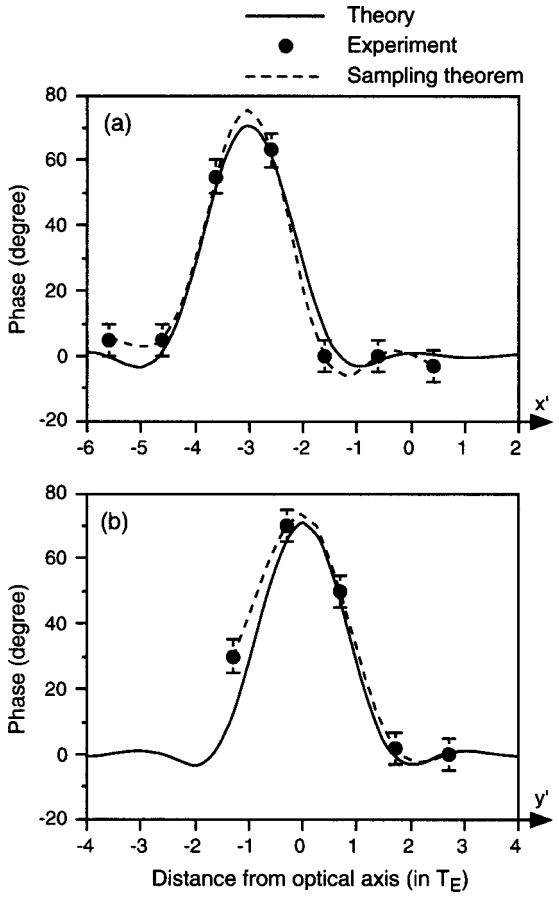

FIG. 5. Phase images of a test dielectric bar with (a) horizontal direction (x') and (b) vertical direction (y') of a two-dimensional image.

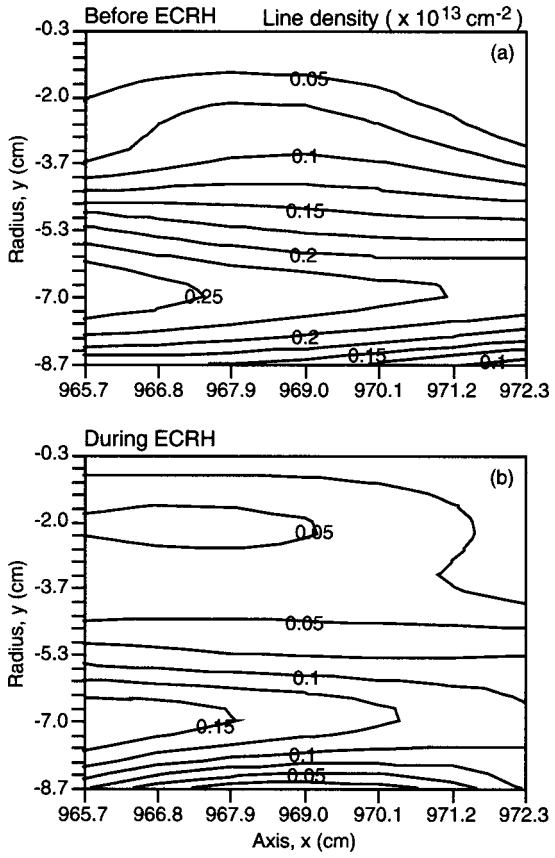

FIG. 6. Measured spatial distribution of the line density at the west-plug cell in the GAMMA 10 tandem mirror at: (a) $t=140$ ms and (b) $t=150$ ms after the plasma buildup. $y=-7.0$ coincides with the center of the plasma.

provided by another IMPATT oscillator (Millitech, IDO-12-R27NBN) with an output of 500 mW. The IF frequency used was 150 MHz. The LO oscillator also provides a signal to be mixed with the probe beam to obtain the reference signal. The quadrature-type detection system[3] provides the phase difference between the two IF signals, with the phase difference being proportional to the line density of the plasma. The detector array used was the imaging array consisting of 4×4, horn antennas with a unit aperture of $1.1\lambda_0\times2.1\lambda_0$, each with waveguides ($0.36\lambda_0\times0.72\lambda_0$, cutoff frequency of 48 GHz) and beam-lead Schottky-diode detectors.[9] The waveguides are used as cutoff high pass filters, since the power of the microwave (28 GHz) for heating plasma is about 150 kW and incident power to the detector is about 1 W and it is necessary to reduce it to below 1 μW. At the other end of the waveguides the beam-lead Schottky diodes were bonded to 4×4 bow-tie antennas, which were monolithically fabricated on a fused-quartz substrate of 38.1×38.1 mm^2. The ion cyclotron range of frequency powers with frequencies of 9.9 and 10.3 MHz (RF1) and 6.36 MHz (RF2) are employed to build up a plasma and heat ions following gun-produced plasma injection. In the plug/barrier cell, two separate 28 GHz gyrotrons are used to heat the plasma. Fundamental electron-cyclotron-resonance heating (ECRH) in the plug region and second-harmonic ECRH in the barrier region produce warm and hot electrons, which are necessary for effective formation of thermal barrier and confining (plug) potentials.

When the ECRH power is applied, the plug potential is created near the position of $z=962$ cm where the magnetic field strength equals 1 T. At the region of $z\geqslant962$ cm, where the imaging system is installed, the loss particles (density) will decrease due to the formation of the plug potential. Figure 6 shows the two-dimensional line-density profiles obtained before and during the ECRH application, respectively, and six shots with good reproducibility and mechanical scanning shot-to-shot of the 4×4 imaging array are used to obtain the two-dimensional image. The size of the plasma (83×67 mm) corresponds to 6×5 pixels on the image plane. For clarity, the images shown in Fig. 6 have been composed of 26×9 pixels by inserting four pixels in the y direction and one pixel in the x direction with the sampling theorem and interpolating linearly. The variation of the profile in the x direction is caused by the change of the magnetic field. It is noted that the density profile in the core region ($r\leqslant-2.3$ cm) decreases during the injection of the ECRH power. This region corresponds to that of the effective confining potential which coincides with the radial profile of the plug-ECRH power deposition. It is also noted that a second maximum appeared at positions $y=-2.0$ cm and $x=967$ cm as shown in Fig. 6(b). The strong ECRH power for potential formation produces the radial electric field in the plasma, and some kinds of diffusion occur in the periphery where the electric field is strong to modify the density distribution. The phase resolution of the interferometer esti-

mated from the fringe noise of the trace is less than 1/200 fringe, where one fringe is equal to the line density of 5.2×10^{13} cm^{-2} at 70 GHz.

The plasma diameter in the central cell of the GAMMA 10 is about 380 mm, and the density distribution using the conventional scanning interferometer was completed by the measured data of 30 mm intervals and 12–13 shots with good reproducibility. Therefore, the spatial resolution in the central cell is 30 mm. On the other hand, since the plasma diameter in the plug region is determined by the square root of the magnetic-field strength ratio, it is about 200 mm due to the ratio being about 1/1.8 of that at the central cell so that the desired resolution in the plug region is about 17 mm. The resolution of 28.7 mm of this optical system appears to be slightly low for the plug region, although it is sufficient for the central cell. If the diameters of all the optical components of the system increase 1.7-fold and the number of pixels increases 1.7-fold, obtaining the desired spatial resolution on the plasma should be possible.

ACKNOWLEDGMENTS

The authors wish to thank Associate Professor J. Bae and Dr. T. Suzuki at Tohoku University for valuable discussions and suggestions. This work was partially supported by a Grant-in Aid from the Ministry of Education, Culture, Sports, Science and Technology of Japan.

[1] K. Uehara, K. Miyashita, K. Natsume, K. Hatakeyama, and K. Mizuno, IEEE Trans. Microwave Theory Tech. **MTT-40**, 806 (1992).
[2] K. Hattori, A. Mase, A. Itakura, S. Miyosi, K. Uehara, T. Yonekura, H. Nishimura, K. Miyashita, and K. Mizuno, Rev. Sci. Instrum. **62**, 2857 (1991).
[3] N. Oyama, A. Mase, T. Tokuzawa, K. Imamura, A. Itakura, T. Tamano, Y. Harada, and K. Mizuno, Rev. Sci. Instrum. **68**, 500 (1997).
[4] H. Soltwisch, Rev. Sci. Instrum. **57**, 1939 (1986).
[5] E. J. Doyle, J. Howard, W. A. Peebles, and N. C. Luhmann, Jr., Rev. Sci. Instrum. **57**, 1945 (1986).
[6] J. Howard, E. J. Doyle, G. Reibeiz, R. L. Savage, Jr., W. A. Peebles, and N. C. Luhmann, Jr., Rev. Sci. Instrum. **59**, 2135 (1988).
[7] J. Howard, Rev. Sci. Instrum. **61**, 1086 (1990).
[8] B. W. Rice, Rev. Sci. Instrum. **63**, 5002 (1992).
[9] D. L. Brower and Y. Jiang, Rev. Sci. Instrum. **66**, 856 (1995).
[10] D. L. Brower, L. Zeng, and Y. Jiang, Rev. Sci. Instrum. **68**, 419 (1997).
[11] T. Tamano, Phys. Plasmas **2**, 2321 (1995).
[12] A. Mase, T. Koseki, A. Itakura, N. Higaki, J. H. Jeong, T. Cho, K. Ishi, and S. Miyoshi, Jpn. J. Appl. Phys., Part 1 **26**, 1867 (1987).
[13] N. Oyama *et al.*, Proceedings of the 8th International Symposium on Laser-Aided Plasma Diagnostics, Doorwerth, 1997, p. 343.
[14] J. Fujita and the LHD Diagnostics Group, *Diagnostics for Experimental Thermonuclear Fusion Reactors*, edited by P. E. Stott *et al.* (Plenum, New York, 1996), p. 617.
[15] B. H. Deng, R. P. Hsia, C. W. Domier, S. R. Burns, T. R. Hillyer, N. C. Luhmann, Jr., T. Oyevaar, and A. J. H. Donne, Rev. Sci. Instrum. **70**, 998 (1999).
[16] P. F. Goldsmith, C.-T. Hsich, G. R. Huguenin, J. Kapitzky, and E. L. Moore, IEEE Trans. Microwave Theory Tech. **MTT-41**, 1664 (1993).
[17] W. J. Smith, *Modern Optical Engineering: The Design of Optical Systems*, 2nd ed. (McGraw–Hill, New York, 1990).
[18] D. B. Rutledge, D. P. Neikirk, and D. P. Kasilingam, in *Infrared and Millimeter Waves*, edited by K. J. Button (Academic, New York, 1983), Vol. 10.
[19] J. W. Goodman, *Introduction to Fourier Optics* (McGraw–Hill, New York, 1968).
[20] P. E. Young, D. P. Neikirk, P. P. Tong, D. B. Rutledge, and N. C. Luhmann, Jr., Rev. Sci. Instrum. **56**, 81 (1985).